Annals of Nuclear Energy 128 (2019) 390–397

Contents lists available at ScienceDirect

Annals of Nuclear Energy

journal homepage: www.elsevier.com/locate/anucene

Transient fission matrix approach for assessing complex kinetics behavior in the ZEPHYR ZPR coupled core configurations

Patrick Blaise [a,*], Axel Laureau [b], Paul Ros [c], Pierre Leconte [a], Kornilios Routsonis [a]

[a] CEA, DEN, DER, Cadarache, 13 115 Saint-Paul-Lez-Durance, France
[b] Ecole Polytechnique Fédérale de Lausanne (EPFL), Switzerland
[c] Institut de Radioprotection et de Sûreté Nucléaire (IRSN), Fontenay-aux-Roses, France

ARTICLE INFO

Article history:
Received 31 August 2018
Received in revised form 5 January 2019
Accepted 17 January 2019
Available online 28 January 2019

Keywords:
Transient fission matrices
Spatial kinetics
ZEPHYR fast/thermal coupled core

ABSTRACT

CEA is currently working on a new ZPR called ZEPHYR (Zero power Experimental PHYsics Reactor), to be built on the Cadarache Center in the next decade. Its awaited experimental capacities should go well beyond traditional needs, and in particular extended possibilities to assess complex 3D kinetics. Transient calculations with accurate neutron kinetics models can be challenged by designing strongly spatially coupled to strongly spatially uncoupled cores with different kinetics constant. An innovative Monte Carlo Transient Fission Matrix (TFM) approach based on fission matrix interpolation model connected to correlated sampling technique has been implemented and applied to the ZEPHYR reference fast/thermal coupled configuration. The model takes into account the redistribution of the power in the core for spatial kinetics (SK) thanks to a local correlated sampling technique developed for this purpose. However, point Kinetics (PK) can be treated as well. The correlated model presented in this paper estimates the coupling coefficients or the influence on the neutron transport of a local variation of different parameters on integral quantities such as k-eff. A dedicated 1D benchmark demonstrates interesting features of this kind of coupled configurations for the validation of complex space-time kinetics transient experiments. A further work will extend this preliminary results to a 2D study case.

1. Introduction

The deep understanding of power reactor behavior during normal and offnormal operation raises the incentive of accurate modeling the transient phases, and large efforts are now deployed by the scientific community to develop and validate complex Multiphysics tools. These (sometimes) strongly coupled codes take into account the interaction between neutronics, providing the fission heating source, and other physics such as the thermal hydraulics and mechanics. Within the multiphysics problem, complex 3D kinetics behavior of coupled cores are one of the most challenging problem to be solved in the near future, both for deterministic schemes, but also for newly developed and implemented methodologies in modern Monte Carlo codes such as TRIPOLI (Brun et al., 2015), Serpent (Leppänen et al., 2015), or MCNP (Brown et al., 2013). Several innovative MTR and technological demonstrator core and reflector designs are characterized by strong geometrical heterogeneities that increase neutron gradient across interfaces, and consequently induce spatial decoupling phenomena. These phenomena, occurring between fissile zones or due to efficient reflector conditions, can be amplified during different transient scenarios, potentially leading to critical situations.

To avoid such situation, validated spatial neutron kinetic models are needed to ensure a limited flux redistribution in the core. Dedicated physical models and numerical resolution algorithms combining precision and acceptable computation time are currently being developed worldwide. In this framework, Monte Carlo methods present an obvious advantage in dealing with complex geometries without adding extra bias in the calculation result. However, some simplifying assumptions in neutron kinetics modeling still have to be made since the increase in computation capabilities is still not sufficient for direct transient Monte Carlo calculations at the full reactor core scale, at least in reasonable times. Deterministic or hybrid approaches may be used, like improved quasistatic methods, but they present drawbacks, as they require regular updates of both power shape and reactivity using full core calculations. However, their potentialities are very interesting and they are still considered as being the standard reference deterministic route for 3D kinetics.

Among Monte Carlo methods, the newly implemented spatial kinetic Transient Fission Matrix (called TFM) approach present

* Corresponding author.
E-mail address: patrick.blaise@cea.fr (P. Blaise).

https://doi.org/10.1016/j.anucene.2019.01.031
0306-4549/

attractive aspects. The methodology is presented in (Laureau et al., 2017; Laureau et al., 2017). The methodology uses discretized Green functions of the Monte Carlo response of the system for performing kinetic calculations. Its main advantage is that it does not require new reference calculation during the transient and thus with a reduced CPU time. Specific interpolation models that generate on the fly estimations of the matrix variations during the transient without requiring new Monte Carlo calculations was also implemented in the TFM module. The correlated sampling technique therein is adequate for treating complex kinetics behavior in fast neutron spectrum heterogeneous cores. The resulting neutronics approach called 'perturbative TFM' is applied in this paper on the ZEPHYR fast/thermal coupled core concept (Blaise et al., 2016; Ros et al., 2017) currently being envisaged to become critical in Cadarache at the horizon 2028.

The present paper will describe the ZEPHYR ZPR project, and in particular its capacity to perform coupled core configurations for large 3D-kinetics transient applications. The TFM methodology is then briefly resumed before going to a direct application of its development on the fast/thermal (MOX-Na/UO_2-H_2O) reference coupled core. The application on a simplified 1D problem will exhibit TFM capabilities to clearly point out coupling coefficients, as a preliminary way to design strong 3D transients in the forthcoming ZEPHYR coupled cores.

2. The ZEPHYR facility

In 2014, CEA started the design of a new versatile ZPR called ZEPHYR (Zero power Experimental PHYsics Reactor), a future facility to be built in Cadarache around 2028, aimed at replacing EOLE and MINERVE with enhanced capabilities. One challenge was to increase its versatility in spectrum adaptation, using fast/thermal coupled core design. The initial goal of such configurations was to measure integral total cross-sections of selected isotopes in a targeted fast spectrum through accurate measurement of reactivity variation using the so-called oscillation technique, historically used in MINERVE (Geslot et al., 2017). Fast-thermal configurations enable to properly reproduce fast spectra using minimum amount of fissile material, taking benefit from the MASURCA fast ZPR and its available fuel stockpile. This versatility also enabled to design fast lattices dedicated to severe accident situations in SFRs (Margulis et al., 2018).

The reference configuration retained for the purpose of our study is composed of a central fast zone built around MOX fast units cells called hereafter ZONA1, initially used for the ERMINE program in the 70's (Ros et al., 2016). These unit cells are made of a mixture of enriched MOx and natural UOx rodlets, within a sodium pellet environment. It is 12 in. high and about 2 in. large. They are zoomed on Fig. 1. This fast lattice enables to reproduce a PHENIX-like spectrum. The core is made of 3 superposed cells (36 in. high), that corresponds to the fissile height. This central fast zone is fed by a peripheral thermal zone, so a basic coupled configuration is obtained. The central radius is adapted in order to avoid any propagation of a central perturbation of oscillated samples to the thermal part, which should induce additional complexity in the sensitivity analysis to the reactivity effect. Furthermore, an adaptation zone made of natural uranium rodlets (smoothing the pure fission neutron spectrum from the enriched ring) was added to optimize the target spectrum in the central channel of the experimental zone, using representativity approach. The complete design process is described in (Ros et al., December 2017). A representation of the 3D geometry in plane (X-Y) obtained with a Monte-Carlo calculation by TRIPOLI-4® (Brun et al., 2015) is presented in Fig. 1.

The ZEPHYR reference fast/thermal core is characterized by strong direct and adjoint spectrum variations as represented in Figs. 2 and 3.

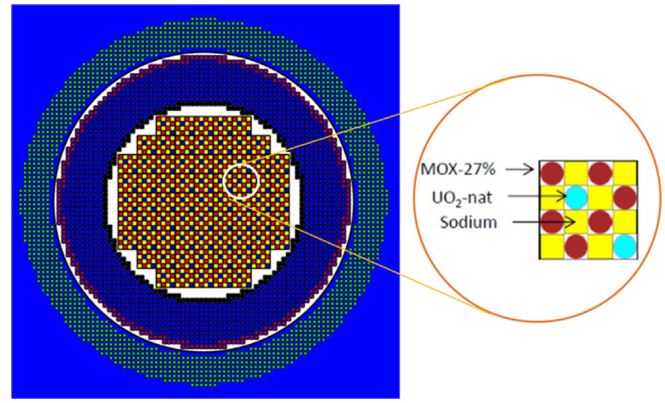

Fig. 1. X-Y representation of the TRIPOLI4® modelling of the Fast/Thermal optimized configuration. *Blue: light water – Green: UO_2 3.7% enrichment – Purple: Metallic U 30% enrichment Navy: natural UO_2 – Black: B_4C absorber – White: Air. The central cells are the one presented in Fig.1.* (For interpretation of the references to color in this figure legend, the reader is referred to the web version of this article.)

As several different zones are coupled, the radial profile of the adjoint flux along the core mid plane, reproduced in Fig. 3 is original and brings the information of two separate fissile zones. This effect will be pinpointed by the TFM approach.

This figure illustrates the importance of the high enriched Uranium ring and the decoupling effect of the transition zone around R = 25 cm. The adjoint calculation was done using the ERANOS system of codes (Rimpault et al., 2002), and is extracted from (Ros, 2017). The TFM plots presented in Section 4 will address these characteristics.

3. Transient fission matrix approach

The Transient Fission Matrix approach is a time dependent version of the fission matrices. Its objective is to precalculate the time dependent transport characteristics of the neutrons in a discretized geometry, in order to perform transient coupled calculations with a reduced calculation time. A clear and complete introduction of the usual fission matrix can be found in (Laureau and Buiron, 2017; Laureau et al., 2017; Laureau, 2015), The raw information contained in any fission matrices $\underline{G}$ is the probability that a fission neutron created in a volume *j* produces a new fission neutron in a volume *i*. This information is then summarized in ad hoc formatted matrices (line *i* column *j*), built according to either prompt (labelled *p*) or delayed (labelled *d*) emission spectra χ, or neutron multiplicities ν, e.g. $\underline{G}\chi_p\nu_p$ as detailed below. The methodology also enables to track average prompt propagation time from *j* to *i* and store the associated information into a dedicated $\underline{T}\chi_p\nu_p$ time matrix. The objective of the present paper being to illustrate a concrete application to coupled core kinetics, interested people are welcomed to read the aforementioned references.

3.1. Prompt and delayed neutrons

Most important phenomena for understanding coupling phenomena are the *prompt-to-prompt* and *prompt-to-delayed* matrices. They can be constructed by tracking and sorting transport probabilities using respective emission spectra χ and neutron production multiplicities ν. Calculations are performed with a Monte Carlo neutronic code using the same approach as for the usual fission matrices with two additional aspects: a link to the type of the neutron at its birth (prompt or delayed) and also to the type of produced neutrons (prompt or delayed). For example the (*i, j*) element of the $\underline{G}\chi_d\nu_p$ matrix contains the probability that a prompt neutron

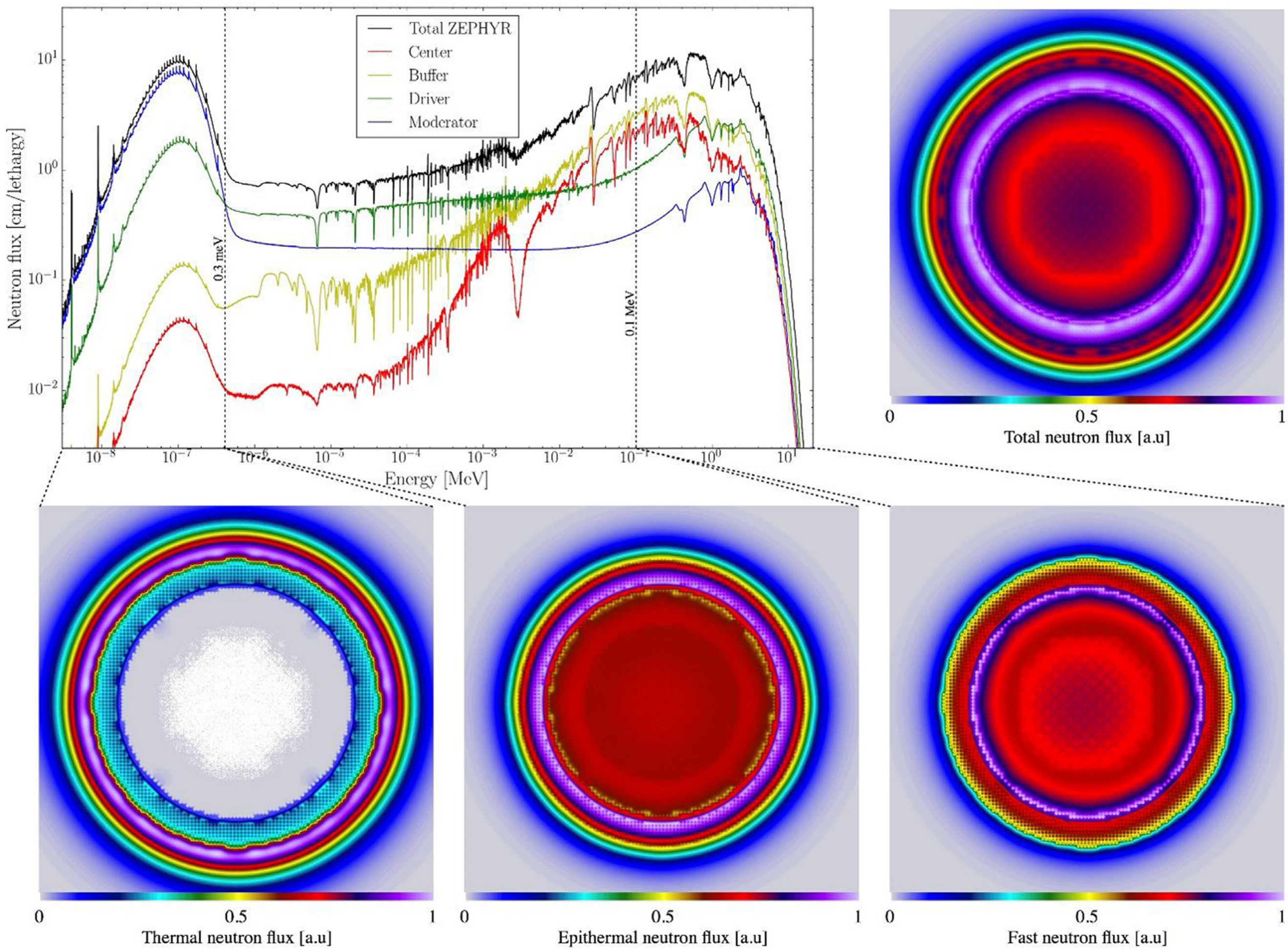

Fig. 2. Neutron spectra in the different areas of ZEPHYR (upper left) together with the neutron flux maps calculated with the Serpent2 code: total flux (upper-right), and thermal/epithermal/fast flux (bottom).

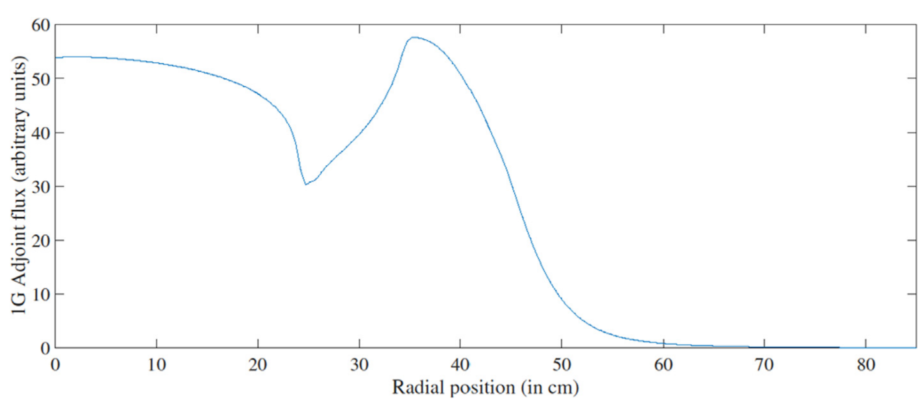

Fig. 3. Radial representation of the 1G adjoint flux in the ZEPHYR fast/thermal coupled configuration.

emitted in volume *j* creates a new delayed neutron per fission in volume *i*. This estimation is done during a ‘classic’ criticality Monte Carlo calculation.

3.2. Temporal aspect

The time-dependent aspect of neutron propagation is second factor required to perform neutron kinetics using TFM. As delayed neutron precursor lifetime is much longer than the neutron transport time, we will only consider the prompt neutron fission to fission time matrix $\underline{T}\chi_p\nu_p$ (delayed neutrons are directly produced after the precursor decay). This matrix contains the average propagation time for a source neutron from *j* to *i*, also evaluated in the same calculation as the matrices.

3.3. Effect of material modification

In order to deal with possible feedback effects during transient calculations, such as temperature (through Doppler broadening or thermal expansion of materials), dedicated interpolation models are required to take into account the modification of the matrices. Previous studies (Laureau, 2015; Laureau et al., 2017) shown that for a reactor with a small migration length (such as a PWR) or with homogeneous areas (such as the liquid fuel reactor MSFR), an interpolation based on reference and perturbed matrices calculations is enough if a capture matrix is added to properly normalize (to one) the number of neutron captures per propagated neutron. However, as shown on Figs. 2 and 3, the ZEPHYR reactor is characterized by strong local variations of direct and adjoint neutron spectra and amplitude. For this reason, a more generic interpolation initially developed in (Laureau et al., 2017) for the heterogeneous ASTRID reactor was used and applied for material density modification, Doppler broadening feedback or concentration variations.

4. Methodology and tools

4.1. Calculation parameters

The TFM matrices are estimated using a modified version of the Serpent2 Monte Carlo code (Leppänen et al., 2015). The associated nuclear data library used is JEFF 3.1.1 (Santamarina et al., 2009). The number of tracked neutrons for each TFM calculation is one billion (10^9). This large amount of particles is mandatory – even for a 1D problem – for obtaining a proper level of convergence on the probabilities plotted in the various matrices.

4.2. ZEPHYR 1D simplified model

The preliminary analysis is performed of the optimized fast/thermal configuration designed in ZEPHYR for fast/thermal coupled configuration, and reproduced on Fig. 4. In order to test the TFM approach, a simplified pseudo-1D benchmark is proposed for the sake of the study. The system boundary conditions for this benchmark is void on the x-radial boundaries in order to reproduce leakage outside the lattice, and reflexion on the z-axial and y-radial boundaries. The fission matrices are calculated along the red rectangle reproduced on Fig. 4b.

Fig. 4a describes the 2D squared geometry from whom the 1D benchmark is extracted (Fig. 4b). Periodicity between the two other axes ensures the 1D characteristics of this model.

The geometry is splitted in 74 meshes as follows:

- Thermal zone: meshes 1–10 (and 65–74 by symmetry)
- Conversion zone: mesh 11 (and 64 by symmetry)
- Transition zone: meshes 12–19 (and 56–63 by symmetry) constituted by nat UO_2 and B_4C (meshes 19 and 56)
- The so-called "ZONA1" cell zone: meshes 20–55

The transient calculation is performed by calculating, for each node, prompts and delayed contributions.

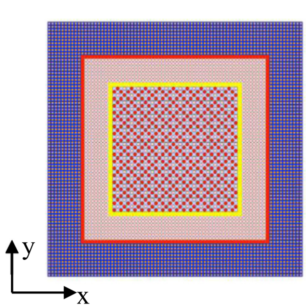

Fig. 4a. Squared 2D representation of the ZEPHYR optimized fast/thermal coupled configuration.

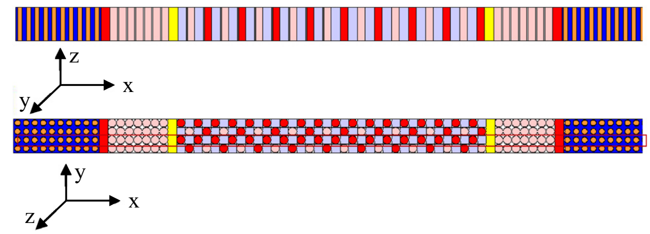

Fig. 4b. Pseudo-1D Traverse of the optimized fast/thermal coupled configuration.

5. Calculation results

5.1. Transient fission matrices

Among all fission matrices that can be generated, four (4) of them were tracked, translating the searched probabilities of producing fission neutrons from one generation to another. The TFM are always plotted as probability that a (prompt or delayed) neutron born in mesh *j* induces a (prompt or delayed) neutron in *i*. The most significant matrix, as it contains the higher number of neutrons, is the «prompt to prompt» matrix, reproduced in Fig. 5. The "delayed to prompt" fission matrix is also reproduced on Fig. 6 for comparison. The color axis reproduces the *propagation probabilities*. It is indicated as $1.e^{-X}$ (to be read as 10^{-X}).

All diagonal terms present important probabilities: numerous fissions appear close to the emission of the "father" neutrons. This is even more exhibited in thermal zones where the diagonal elements are even tighter (more peaked), being a consequence of shorter neutron mean free paths. The case of metallic uranium is interesting as being non-symmetrical (ie the probability of producing a new prompt neutron is not spatially symmetrical). The U_{met} fuel is the source of mainly all fission neutrons (mesh 11). Few fission appear either in the fast zone, or in the thermal buffer zone. A reading of line 10 (target bin) shows that the probability exhibits asymmetries (prompts neutrons emitted from the central fast zone propagates further to create prompt neutrons in the enriched U rodlet). Starting from column 11, almost no neutron in the central meshes is produced from initial neutron from the conversion zone. Hence, the "prompt to prompt" matrix mostly points out strongly decoupled cores.

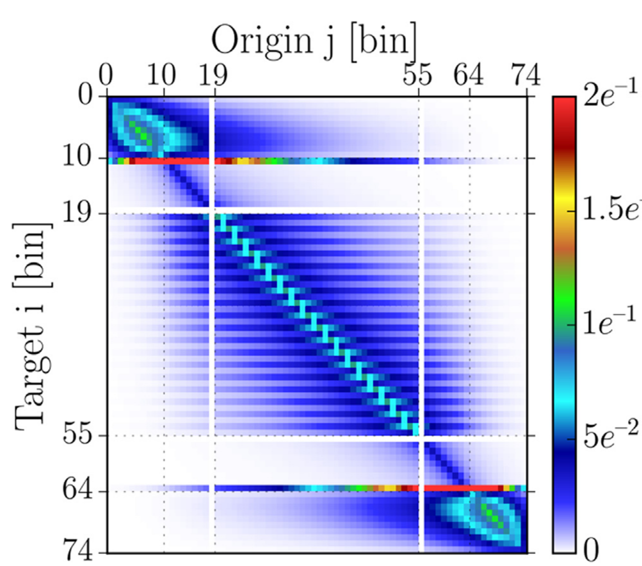

Fig. 5. «Prompt-to-prompt» fission matrix.

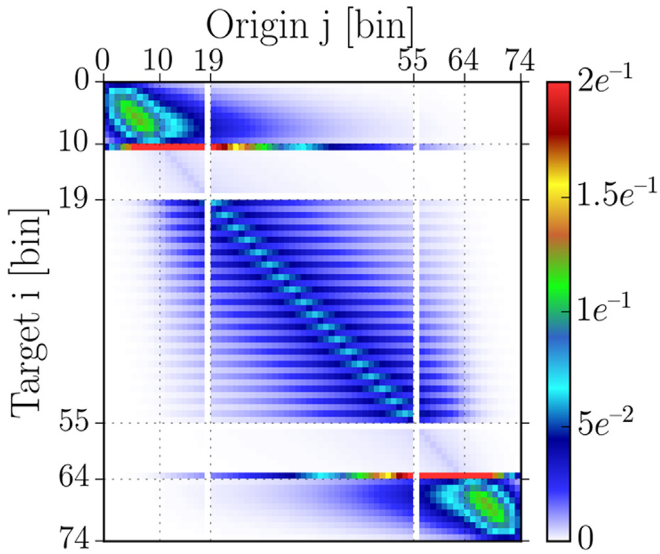

Fig. 6. «Delayed-to-prompt» fission matrix.

The other fission matrices linked to delayed neutrons are presented in the next Figs. (8,9). A qualitative interpretation of their particularities is made. The main difference between those matrices and the prompts ones comes from meshes 12–18 (natural UO_2) where emission probabilities tend to zero. This particular behavior mainly comes from dephasing between delayed neutron spectra, whose average energy is lower than the prompt neutrons, and the "fertile" nature of the medium, mainly composed of ^{238}U. In fact, the average energy of the delayed "father" neutrons is much lower than the 1 MeV fission threshold (average energy is around 300–400 keV), and hence do not produce fissions.

Delayed neutrons population being much lower than prompt neutrons population, the associated probabilities are of smaller amplitude. Throughout isotopes present in the core, uranium isotopes present the highest delayed neutron fractions. Again, one observes higher probabilities between meshes 12–18, thanks to the presence of ^{238}U. Inversely, the spread around the main diagonal is more restricted than previously, in particular around the

Looking carefully to fast/thermal decoupling, it is noteworthy to observe that the probability to generate fissions in the core center is very low (less than 1%), except for fission neutrons coming from a fission into a fast ZONA1 cell. If the probability to generate a fission neutron in the core center from a neutron born in the nat-UO2 of the adaptation zone is not negligible, it has to be weighted by the low proportion of neutrons born in this core area. The adjoint transport operator, being a picture of the adjoint flux (see Fig. 3), can be extracted from a column readings for each line. Considering fission in a given mesh, the associated columns give the origin of the fission neutron, hence the importance of this neutron. For example, a lecture of line *i* = *37* shows that fission neutron produced in the core center are mainly issued from the ZONA1 cells.

The decoupling is clearly observed on the 1D traverse of the prompt to prompt matrix eigenvector corresponding to the first (largest) eigenvalue – ie the fundamental mode (Fig. 7). At the periphery, the eigenvector follows a thermal flux shape (zone 1), with a peak corresponding to the enriched uranium rods (zone 2). After the adaptation zone (3), characterized by a very low importance (hence low associated eigenvector), the neutron flux stabilizes on the fast domain with a flat cosine shape (4).

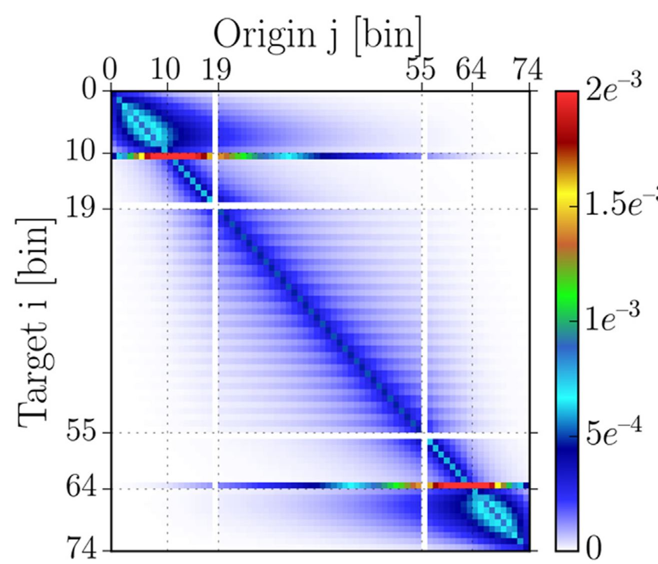

Fig. 8. «Prompt-to-delayed» fission matrix.

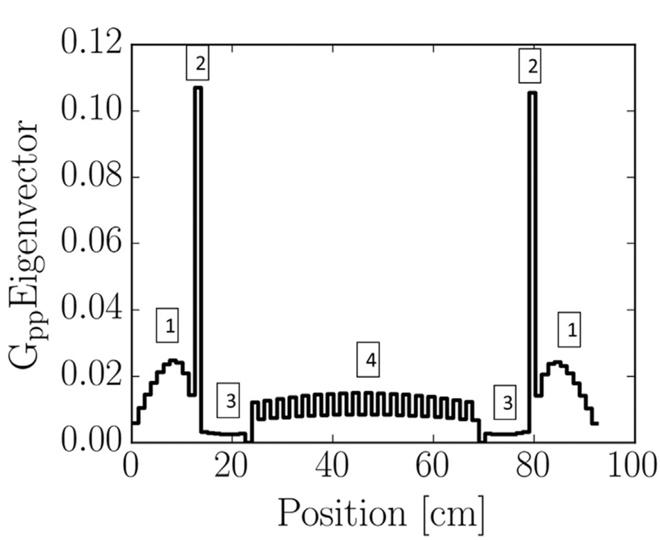

Fig. 7. «Prompt-to-prompt » fission matrix eigenvector.

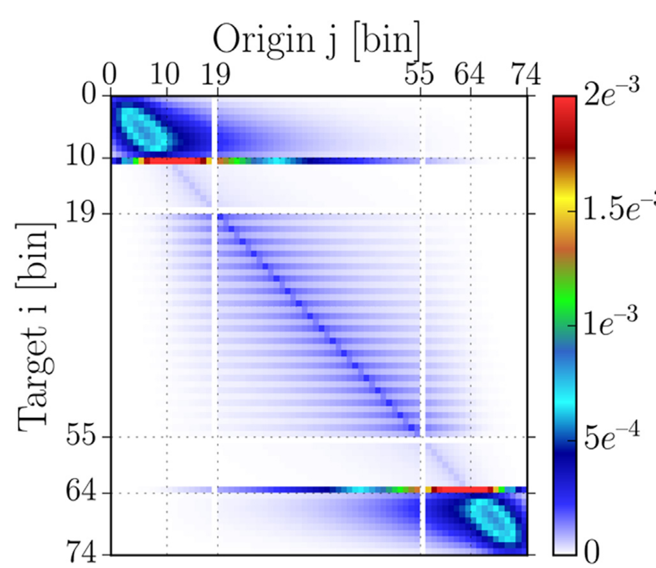

Fig. 9. . «Delayed-to-delayed» fission matrix.

ZONA1 cells, due to a lower delayed neutrons fraction of the plutonium isotopes.

Fig. 9 mainly focuses on delayed neutrons fission matrix. It presents very weak probabilities in the core center, mainly due to the presence of plutonium isotopes, as well as « holes » in natural UO_2 thanks to non correspondence between the main delayed neutron spectrum energy (few hundreds of keV) and the ^{238}U threshold fission cross section. In conversion and thermal zones, high values are obtained, as those zones are mainly composed of enriched uranium material.

Fig. 10 reproduces the $\underline{T}\chi_p\nu_p$ time operator of the « prompt to prompt » events. Average prompt neutrons lifetimes present strong differences and extend to two decades. This extension is due to the coupling of thermal and fast zones, through strongly different spectra.

The correlation between mean spectrum energy and neutron lifetime is obvious neutrons become thermal through a time expensive multiple scattering process.

This matrix also points out that neutrons from the thermal zone and fissioning in the thermal zone, as well as neutrons from the fast zone which will produce a fission in the thermal zone are characterized by the largest lifetime (above 10 μs): they are illustrated by red bands on the upper and lower parts (arrival meshes 1–10). Within the fast zone (meshes 12–64), neutron lifetimes are shorter as neutrons issued from the fast zone induce fission as they are still fast. However, one can observe a slight difference in mesh 11, where neutrons from the ZONA1 zone have to go through the whole conversion zone to induce fission in the enriched metal uranium. Neutrons issued from the thermal zone and making a fission in the central fast zone (originating from meshes 1 to 10 and 65 to 74) have a low lifetime: only fast neutrons from the thermal zone are able to cross the conversion zone. This has to be linked also to the asymmetry pointed out in Fig. 5 (as well in all other matrices).

5.2. Material perturbation and impact on the fission matrices

Local and global perturbations are directly treated through TFM approach. We will here after give two examples related to sodium rodlets present in the geometry. The first one illustrates the effect on a negative global perturbation of the sodium density of −1%, captured by both correlated sampling (implemented in (Laureau et al., 2017) and independent Monte Carlo calculation. The perturbation on the ($\nu_p \rightarrow \chi_p$) probability is plotted on Fig. 11.

Several observations can be made:

- The correlated sampling approach exhibits better convergence on the propagated perturbation,
- The impact of the Na perturbation on the fission probability is reduced on the main diagonal, meaning that the fission probability is lower than in the reference case. In fact, the phenomenon is linked to the higher mean free path of neutrons propagating in less dense medium. When the sodium density decreases, the neutrons scatter further in the geometry, hence locally reducing the fission probability.

The local perturbation effect of the sodium density on the overall propagation probabilities can be plotted. Fig. 12 reproduces a perturbation of the sodium density close to the fast/transition zone interface, and its impact on the prompt-to-prompt neutron propagation probability (the unperturbed reference is Fig. 5).

Several zones (1 & 2) around the perturbation must be explained.

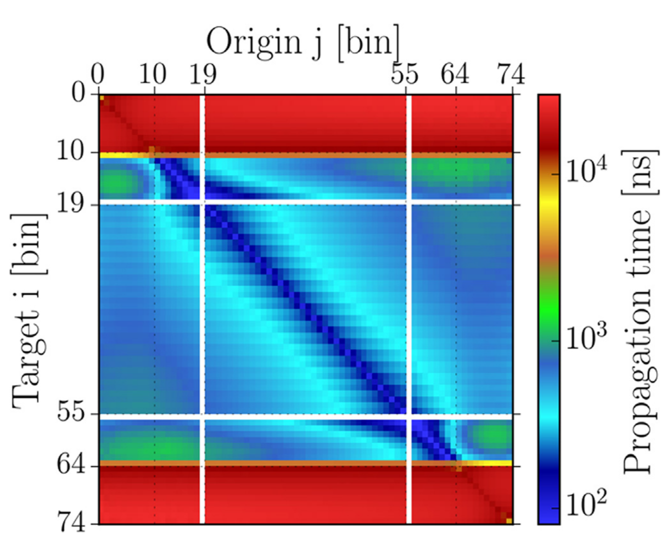

Fig. 10. "Prompt to prompt" time operator matrix, giving the propagation time (in ns).

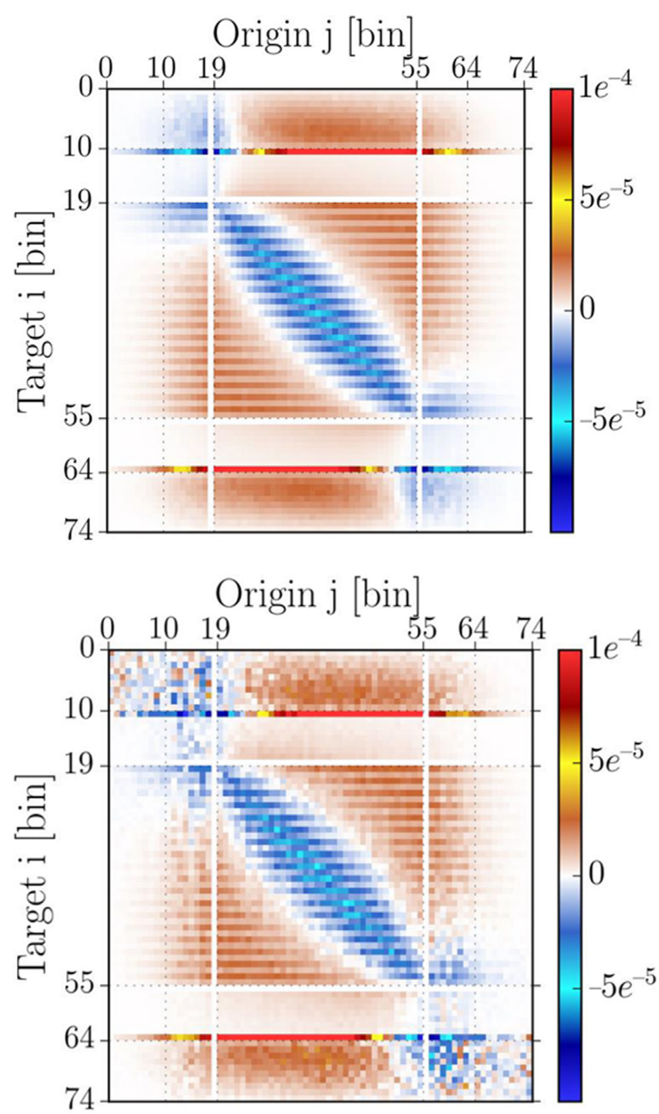

Fig. 11. "νp → χp" (prompt-to-prompt) discrepancy between two states by independent Monte Carlo approch (up) and correlated sampling (down).

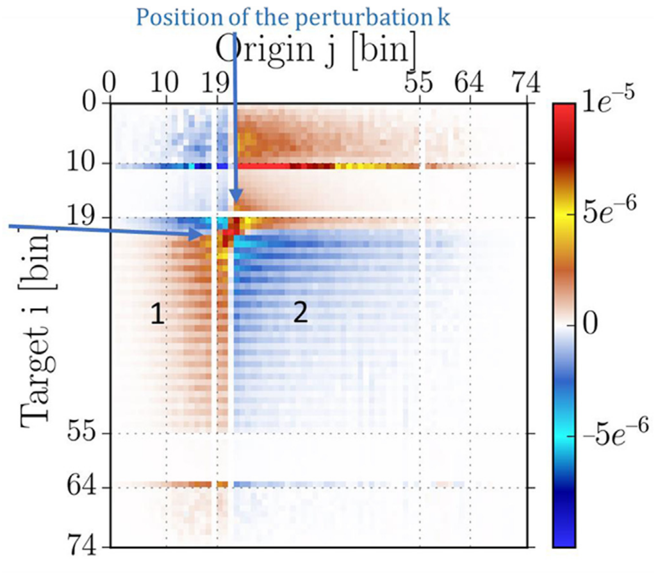

Fig. 12. Local impact of a 1% negative perturbation in the sodium density on the prompt-to-prompt fission probabilities.

Case 1: if the position of the perturbation k (called hereafter "bin") is between the emission position j and the fission position i ($i < k < j$) or-($j < k < i$), then the neutron crosses the perturbation and has higher probability to pass the perturbed bin without scattering and losing energy, thus leading to (on average) higher energy neutrons arriving in bins after the perturbation (leading to more fissions in the MOX). The corresponding mean free path increases due to the density decrease.

Case 2: if (i and j) < k or (i and j) > k, then the proportion of neutrons having crossed the perturbed area having less probability to scatter back, the fission probability decreases accordingly in j and i.

Fig. 13 reproduces the evolution of the local perturbation as it crosses the geometry. This perturbation displacement is easily illustrated by plotting the radial sensitivity profile of the ZEPHYR benchmark eigenvalue, also reproduced on Fig. 14. The sensitivity is calculated as the difference between the eigenvector of the reference situation and the same eigenvector in the perturbed situation, relative to the total reactivity effect (calculated as $k_{pert}/k_{ref}-1$).

Fig. 14 depicts an example of the total (fundamental mode) eigenvector perturbation. Each column represents the eigenvector perturbation due to a local Na perturbation. The sum represents the overall perturbation of the central area. The eigenvector-perturbed matrix exhibits a clear trend to bring back the fissions

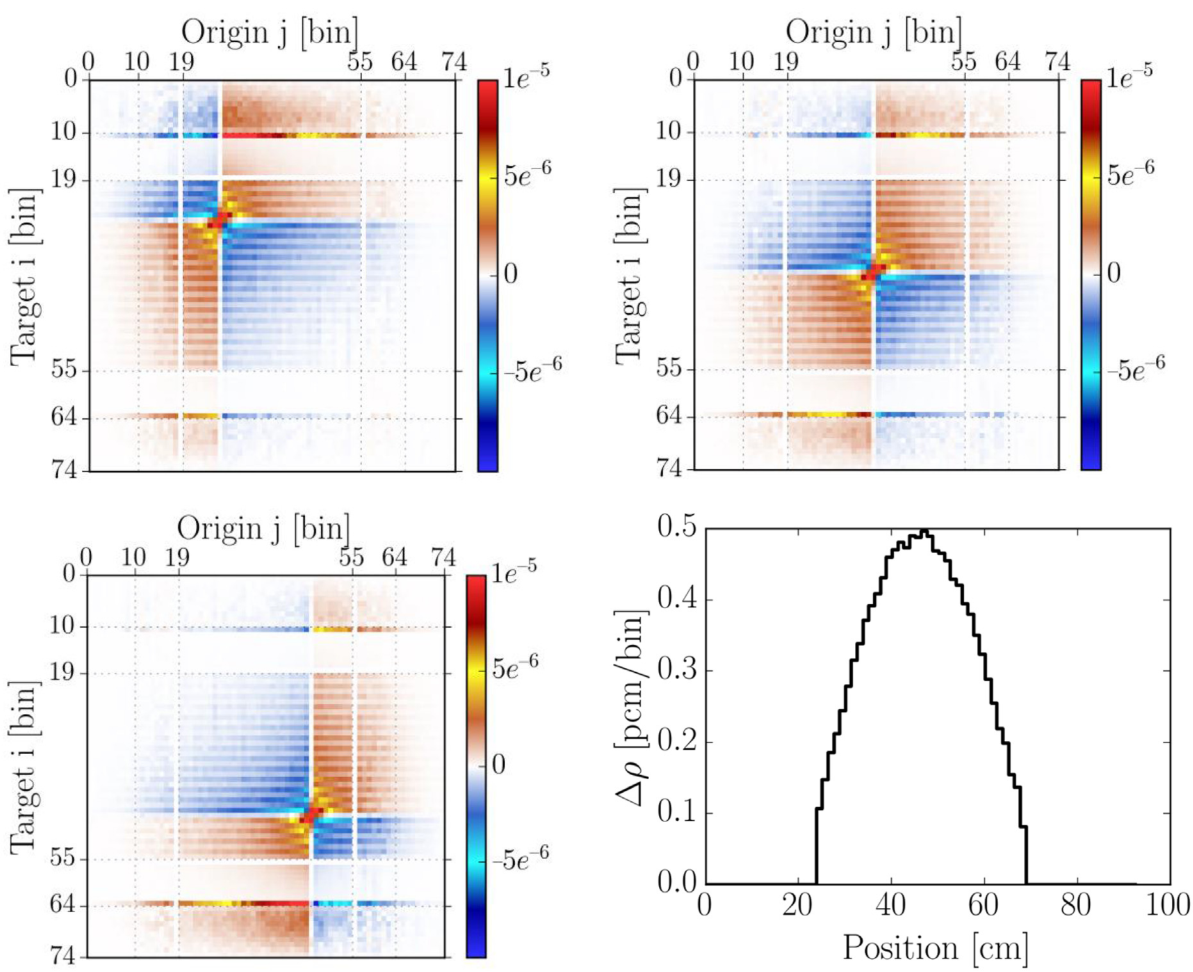

Fig. 13. Evolution of the fission matrix propagated probability as the density perturbation crosses the geometry (left). The sensitivity profile of the reactivity per perturbed bin (overall effect) is also reproduced (bottom right).

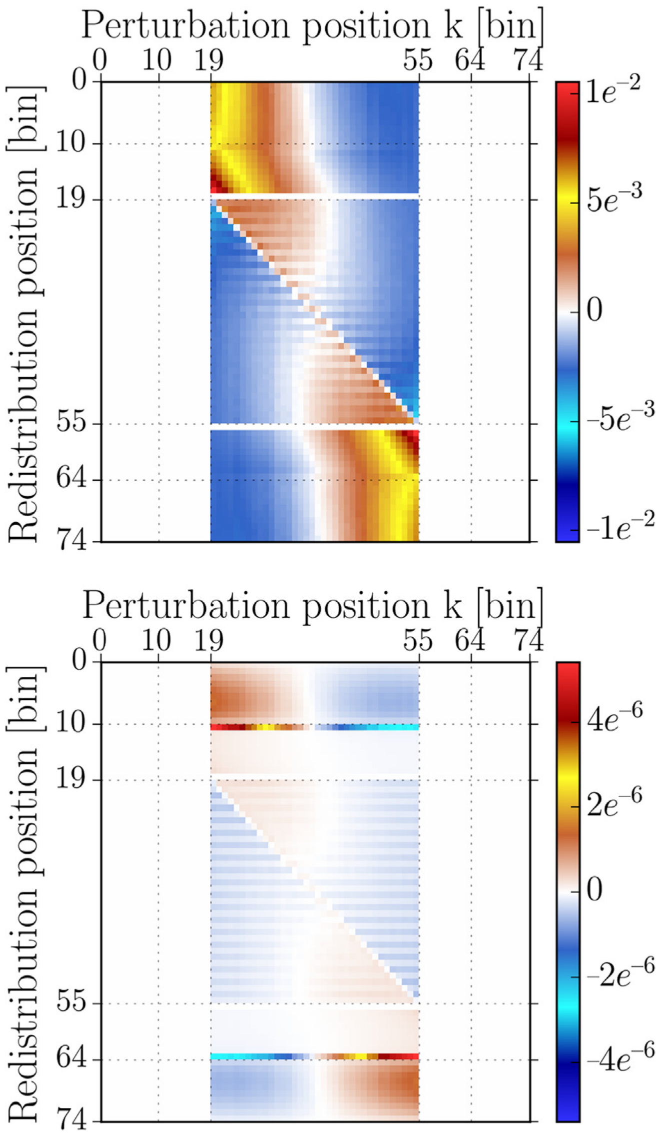

Fig. 14. Eigenvector matrix redistribution due to the total Na perturbation. Up: perturbation on the eigenvector (in %) – Down: normalized perturbation per bin.

to the perturbed side, with a strong local discontinuity where the perturbation occurs.

6. Conclusions

A TFM approach was applied on a simplified coupled core 1D benchmark. Fission matrices as well as the temporal operator matrix are full of information for the purpose of the future ZEPHYR ZPR. They enable the physicist to qualitatively illustrate neutron coupling or decoupling effects between zones in strongly heterogeneous configurations, characterized by large delayed neutron fractions. Used as a complement to the coupling theories of Avery (Avery, 1958) and Kobayashi (Kobayashi, 1998), they are a powerful tool for the physical analysis of complex transients. An extension of the TFM approach will be used in the near future to enlarge the ZEPHYR capabilities for exhibiting large coupling/decoupling effects, with the aim to build dedicated programs for full 3D transient programs in high dominant ratio geometries. In particular, the TFM will be implemented in the TRIPOLI-4© MC code, and compared to multipoint approaches to solve complex 3D kinetics problems, as flux tilts in large cores.

References

Avery, R., 1958. Theory of coupled reactors. In: Proc. 2nd United Nations Conf. for Peaceful Use of Atomic Energy, United Nations. Vol. 12. p. 182.

Blaise, P., Boussard, F., Ros, P., Leconte, P., Margulis, M., Martin, G., Blandin, K., March 2016. Experimental R&D innovation for Gen-2,3 & IV neutronics studies in ZPRs: a path to the future ZEPHYR facility in Cadarache. In: Proc. Int. Conf IGORR. Berlin.

Brown, F.B., Carney, S.E., Kiedrowski, B.C., Martin, W.R., 2013. Fission Matrix Capability for MCNP Monte Carlo, Supercomputing in Nuclear Applications and Monte Carlo 2013, Paris, Oct 27-31, LA-UR-13-26962.

Brun, E., Damian, F., Diop, C., Dumonteil, E., Hugot, F., Jouanne, C., Lee, Y., Malvagi, F., Mazzolo, A., Petit, O., et al., 2015. Tripoli-4®, CEA, EDF and AREVA reference Monte Carlo code. Ann. Nucl. Energy 82, 151.

Geslot, B. et al., 2017. A hybrid pile oscillator experiment in the Minerve reactor. Ann. Nucl. Energy 108, 268–276.

Kobayashi, 1998. A relation of the Coupling coefficient to the eigenvalue separation in the coupled reactors theory. Ann. Nucl. Energy 25 (4–5), 198–201.

Laureau, A., 2015. Développement de modèles neutroniques pour le couplage thermohydraulique du MSFR et le calcul de paramètres cinétiques effectifs. Université Grenoble Alpes.

Laureau, A., Buiron, L., Fontaine, B., 2017. Towards spatial kinetics in a low void effect sodium fast reactor: core analysis and validation of the TFM neutronic approach. EPJ Nucl. Sci. Technol. 3, 17.

Laureau, Buiron, L., Fontaine, L., 2017. Local correlated sampling Monte Carlo calculations in the TFM neutronics approach for spatial and point kinetics applications. EPJ Nucl. Sci. Technol. 3, 16.

Laureau, A., Buiron, L., Fontaine, B., Pascal, V., April 16–20, 2017. Fission Matrix Interpolation for the TFM Approach Based on a Local Correlated Sampling Technique for Fast Spectrum Heterogeneous Reactors. In: Proc. Int.Conf. M&C 2017, Jeju, Korea.

Laureau, A., Heuer, D., Merle-Lucotte, E., Rubiolo, P., Allibert, M., Aufiero, M., 2017. Transient coupled calculations of the molten salt fast reactor using the transient fission matrix approach. Nucl. Eng. Des. 316, 112–124.

Leppänen, J., Pusa, M., Viitanen, T., Valtavirta, V., Kaltiaisenaho, T., 2015. The Serpent Monte Carlo code: status, development and applications in 2013. Ann. Nucl. Energy 82, 142.

Margulis, M., Blaise, P., Gilad, E., 2018. Modeling representative Gen-IV molten fuel reactivity effects in the ZEPHYR fast/thermal coupled ZPRs. Part I—Assembly level. Int. J. Energy Res., 1–23

Rimpault, G., et al., 2002. The ERANOS code and data system for fast reactor neutronic analyses. In: PHYSOR Conference, Seoul, Korea.

Ros, P., Sept. 2017. Conception neutronique de configurations expérimentales à forte adaptation spectrale en réacteur de puissance nulle pour des applications multi-filières Gen-II,III & IV" (PhD Thesis). (on-line https://tel.archives-ouvertes.fr/tel-01689821).

Ros, P., Blaise, P., Leconte, P., Doger de Spéville, H., Maillot, M., 2017. Fast-thermal coupled cores in ZPRs: a demonstration of feasibility and pertinence for the ZEPHYR project. Ann. Nucl. Energy 110, 290–305.

Ros, P., Leconte, P., Blaise, P., Sept 2016. Integral cross sections of fission products in fast reactors. Re-interpretation of the ERMINE V experiment: Interest of Fast-Thermal Coupled Cores. In: Proc. Int. Conf ND2016, Brugges.

Santamarina, A., et al. 2009. The JEFF-3.1.1 Nuclear Data Library, JEFF Report 22, OCDE.